JOURNAL OF MARITIME RESEARCH

Vol XXII. No. I (2025) pp 371–377

ISSN: 1697-4840, www.jmr.unican.es

Effectiveness of Breakwater Design to Reduce Wave Height and Energy Using 2D Numerical Model in Ulee Lheue Port Area, Banda Aceh

S. Purnawan[1], Rizwan Thaib[2,*], Koko Ondara[3], Guntur Adhi Rahmawan[4]

ARTICLE INFO

Article history:
Received 23 Aug 2024;
in revised from 30 Aug 2024;
accepted 17 Sep 2024.

Keywords:
numerical model; Ulee Lheue;
breakwater; fishing port; design.

ABSTRACT

Ulee Lheue Port, a vital economic hub in Banda Aceh, faces operational challenges due to wave and current disturbances in its harbor area. To mitigate these adverse effects and ensure safe and efficient port operations, this study investigated the effectiveness of various breakwater configurations. To achieve this, we employed a 2D numerical model utilizing the Flow Model FM application and analyzed crucial data, including the water depth, tide, and wind patterns. We simulated three distinct scenarios for the coastal protection structures. In Scenario 1, a single breakwater structure was implemented, while Scenario 2 featured two structures positioned at the northern and southern entrances of the harbor. Scenario 3 closely resembled Scenario 2, but included only one structure on the northern side. The results demonstrated that breakwaters can significantly reduce wave heights and current speeds, with the two-breakwater configuration proving to be the most effective. In this scenario, the maximum current speed, wave height, and average wave energy were reduced by 28 %, 87%, and 56 %, respectively. These findings highlight the crucial role of breakwaters in enhancing the safety and efficiency of operations at the Ulee Lheue Port, providing a valuable tool for coastal infrastructure planning and management.

1. Introduction.

The fishing industry is essential for providing food and driving economic growth by employing a significant number of people, including both fishermen and support staff. Fishing ports are the heart of fishing communities and crucial for the industry's sustainability (N'Souvi et al., 2023; Thaib et al., 2024). They support fishing activities and the distribution of catches while also enabling accurate catch records that aid in responsible fisheries management and sustainability (Feng et al., 2024). Effective port operations depend on an adequate land-based infrastructure and optimal water conditions for safe and efficient loading and unloading. Safe navigation requires sufficient depth and calm water for smooth handling (Gao et al., 2017; Hou et al., 2021; Romano-Moreno et al., 2022).

Breakwaters are essential coastal structures that provide sheltered harbors and calm basins to protect coastal areas from waves and storms (Akbari et al., 2022; Guler et al., 2024). They also play a crucial role in safeguarding ships and ensuring safe berthing (Hou et al., 2021; López and Iglesias, 2014). However, it's important to note that breakwaters can influence local hydrodynamics, potentially impacting sediment transport and nearshore regimes (Abood et al., 1999; Dev et al., 2023; Paravath et al., 2021). An effective breakwater can reduce the wave height and shield against severe storms while minimizing the environmental impacts (Archetti and Zanuttigh, 2010; Tsai et al., 2024). Engineers use numerical modeling to refine breakwater designs and simulate wave and current behaviors to ensure that structures are both effective and environmentally friendly (Cui et al., 2021; Ondara et al., 2018; Wang and Reeve, 2010; Zhao et al., 2022). This model helps guarantee that breakwaters can withstand real-world conditions and provide adequate protection for coasts and ports.

[1]Department of Marine Sciences, Faculty of Marine and Fisheries, Universitas Syiah Kuala, Indonesia.
[2]Universitas Syiah Kuala. Indonesia.
[3]Fish Quarantine and Inspection Agency. Indonesia
[4]Kementerian Kelautan dan Perikanan Republik Indonesia.
*Corresponding author: Rizwan Thaib. E-mail Address: rizwanthaib@usk.ac.id.

Banda Aceh, located on the western coast of Indonesia, is positioned near the convergence of the Indian Ocean, Malacca Strait, and Andaman Sea (Haditiar et al., 2024). This region features a diverse marine environment with significant fisheries potential (Haridhi et al., 2018; Purnawan et al., 2023). The waters around Banda Aceh support many local fishers engaged in small-scale fishing, particularly in the Ulee Lheue sub-district, which is vital to their livelihoods (Fadli et al., 2021).

Figure 1: Bathymetric Map of Ulee Lheue, Banda Aceh City, Indonesia.

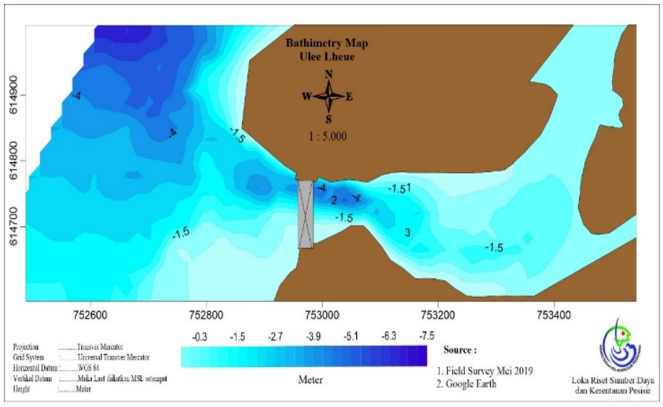

Source: Authors.

The conditions at the Ulee Lheue port (Figure 1) present significant challenges for fishing boats, including high waves, strong currents, and sedimentation issues (Fatimah and Fauzi, 2021; Rahmawan et al., 2021). Despite these obstacles, the port of Ulee Lheue remains crucial for supporting the fishing and marine industries in Banda Aceh City, contributing significantly to the local economy. Constructing breakwaters as coastal protection structures is considered a viable solution to mitigate these challenges. This study explores the design and placement of breakwaters to dampen waves and currents using three proposed scenarios. Numerical modeling was used to evaluate each scenario and identify the most effective design for the conditions at the Ulee Lheue port (Ahn et al., 2019). By employing the Flow Model FM application, our numerical model not only predicts outcomes but also offers validated solutions readily applicable to real-world scenarios at Ulee Lheue Port.

2. Matherials and Method.

2.1. Numerical Modeling Approach.

To evaluate the effectiveness of various breakwater configurations, a two-dimensional (2D) numerical modeling approach was employed. The study area was centered on the port of Ulee Lheue, with a specific observation point located at 95.28309° longitude and 5.55749° latitude. The numerical model utilized the Flow Model FM application, which solved the 2D shallow water equation and depth-integrated Navier-Stokes equation.

We utilized direct measurement data, including tidal and bathymetry data, in addition to supportive information from Topex satellite data with a 1250 × 1250 resolution, captured every 60 min. Shoreline data were obtained from Google Earth images, while wind data were collected hourly from the BMKG station situated at 95.41700° longitude and 5.52244° latitude.

2.2. Model Setup.

The spatial domain of the model was defined using an unstructured mesh with linear triangular elements (Pradhan et al., 2020). Tidal data for the simulations were sourced from verified satellite data and direct measurements from the Ulee Lheue Port. Tidal harmonic principal component analysis and Formhzal number determination were performed using the least-squares method. The parameters of the current and wave models are listed in Table 1.

Table 1: Simulation input parameters.

Parameter	Description
Flow model input	
Time	No of time step= 320
	Interval = 86400 s
Periode	1/1/2016 0:00:00 to 30/10/2016 00:00:00)
Equation	- High order
	- CFL = 0,8
	- Density Barotropic
	- Viscosity = Constant Smagorinsky formulation 0,28
Wind Forcing	- 1/1/2016 0:00:00 to 30/10/2016 00:00:00)
	- Constant friction 0,001255
Tidal	- Predicted
	- Analysis input tidal potential
	- Varying in time and along boundary
	- 1/1/2016 0:00:00 to 30/10/2016 00:00:00)
Wave model input	
Basic Equations	- Fully spectral formulation
	- Instationary formulation
Equation	- Low order geographical
	- Logarithmic discretization
	- No diffraction
	- Quadruplet wave interaction
	- gamma form wave breaking
Initial conditions	- JONSWAP fetch growth
Current	- Hidrodynamic model (u,v)
	- Varying in time and domain
Wind forcing	- per 3600 s (1/1/2016 0:00:00 to 30/10/2016 00:00:00)
	- Varying in time and constant domain
	- Coupled air sea
	- Background Charnock = 0,01
Tidal	- Predicted
	- varying in time and domain
	- per 3600 s (1/1/2016 0:00:00 to 30/10/2016 00:00:00)

Source: Authors.

2.3. Simulation Parameters.

To comprehensively evaluate our designs, we delineated three distinct scenarios, each intended to test a specific breakwater configuration's impact on wave dynamics. Scenario 1 consisted of a single oval structure adjacent to the jetty. In scenario 2 consist of two structures, one near the jetty to the north and another in front of the river mouth to the south. In Scenario 3, a single structure was positioned on the north side, similar to the northern structure in Scenario 2. All breakwaters were modeled as impermeable structures to absorb wave energy and prevent wave run-up and overtopping

Numerical simulations were performed from January 1st to November 30, 2016, providing output data on the current direction, velocity, wave height, and direction. During these simulations, the breakwater structures were modeled as impermeable

to absorb all wave energy and to prevent wave run-up and overtopping (Hsu et al., 2004; Huang et al., 2003; Zhou et al., 2023). They have been shown to be effective in protecting coastal areas by reducing wave height and controlling surface current velocity (Kim et al., 2014; Rupali and Kumar, 2021). In this study, 2016 was selected because of the availability of comprehensive and reliable data, which ensured the accuracy of the research results.

2.4. Breakwater Design.

The breakwater height in the study area was determined by incorporating bathymetry, waves, and tidal data (Samaras et al., 2013; Takagi and Goda, 2000). The predicted water levels for the next 20 years (Ghose et al., 2010) estimated that the water height would reach 1.31 meters above the mean sea level during high tide and fall to -1.11 meters below the mean sea level during low tide. Additionally, the maximum projected wave height was calculated at 1.61 meters, with a wave period of 3.6 seconds. To include a safety margin, an additional 50 cm was added to the breakwater elevation in all scenarios. This resulted in a final breakwater height of 3 m from the water surface to the crest during the design mean sea-level condition.

In Scenario 1, the design features a single oval-shaped structure adjacent to the jetty, comprising three segments, each 20 m long and 10 m wide, at the Mean Sea Level (MSL), resulting in a total length of 60 m (Figure 2a). Scenario 2 included two structures (Figure 2b); the northern structure measured 130 m in length, whereas the southern structure was 120 m long, with both having a width of 10 m at the MSL. Scenario 3 was similar to Scenario 2, with a single structure positioned on the north side, identical in dimensions and location to the northern structure in Scenario 2 (Figure 2c).

Figure 2: Dimensional design of breakwater structures: (a) Scenario 1, (b) Scenario 2, and (c) Scenario 3 consists of only the north structure (identical to the north structure in Scenario 2). The figure outlines the spatial arrangement and relative dimensions of each breakwater structure within their respective scenarios.

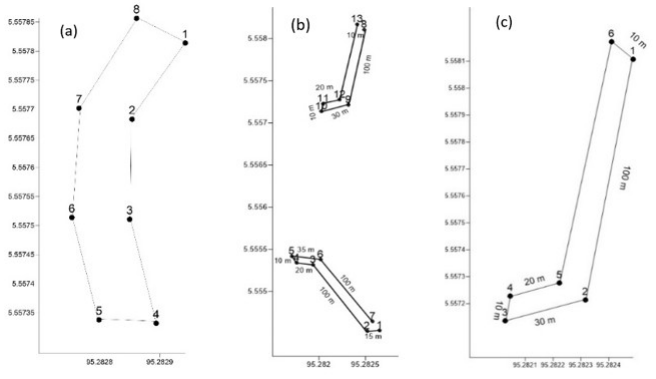

Source: Authors.

Cross-sectional profiles of each breakwater were developed to illustrate the elevation and interaction between the sea surface and seabed (Figure 3). Notably, in Scenario 2, the northern breakwater reached a maximum depth of 2.98 meters at its center and 1.9 meters at its end (Figure 3b). Meanwhile, the southern breakwater, depicted in Figure 3c, exhibited a maximum depth of 0.56 meters at its end. This area is particularly susceptible to sedimentation, resulting in shallow water depths where the southern breakwater is located.

Figure 3: Cross-sectional profiles of breakwater structures: (a) Scenario 1, (b) Scenario 2, and (c) Scenario 3. The diagrams illustrate the elevation and structural design and show the interaction between the breakwater crest, sea surface, and seabed in each scenario.

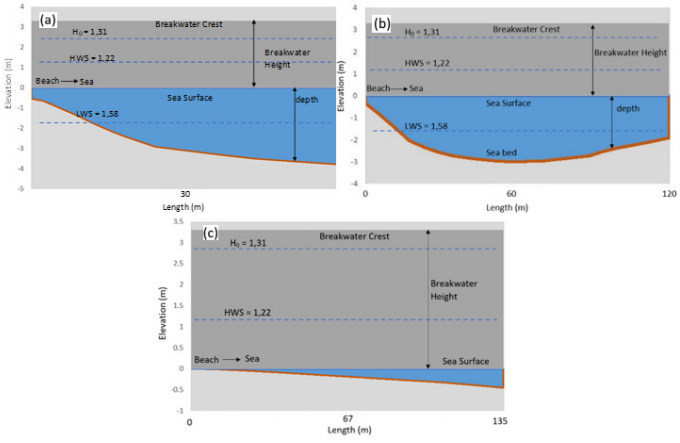

Source: Authors.

3. Results and Discussion.

To evaluate the effectiveness of the three breakwater scenarios, their effects on the current velocity, wave height, and energy were compared to the existing conditions. Numerical simulations were conducted from January 1st to November 30, 2016, and provided data on the current direction, velocity, wave height, and direction. The breakwater structures were modeled as impermeable to absorb all wave energy and to prevent wave run-up and overtopping.

3.1. Current Velocity Reduction.

Under existing conditions, the maximum current around the jetty was measured at 9.34 cm/s, flowing from the north towards the jetty. Conversely, the current from the south, directed towards the river mouth, was redirected towards the pier before following the natural coastline morphology northward (Figure 4a).

With the introduction of the structures in Scenario 1 (Figure 4b), the maximum current decreased to 7.5 cm/s. Initially, this current moved eastward into the estuary but later changed direction to follow the coast. The presence of the breakwater led to a weakening of the northern current, which was deflected towards the structure, while the remaining flow continued parallel to the shoreline.

In Scenario 2 (Figure 4c), the maximum recorded current was 8.3 cm/s. A portion of the water mass moved eastward

Figure 4: Current conditions for full tide: (a) Without structure under existing conditions. (b) Scenario 1 with the proposed structure. (c) Structure of Scenario 2. (d) structure in scenario 3.

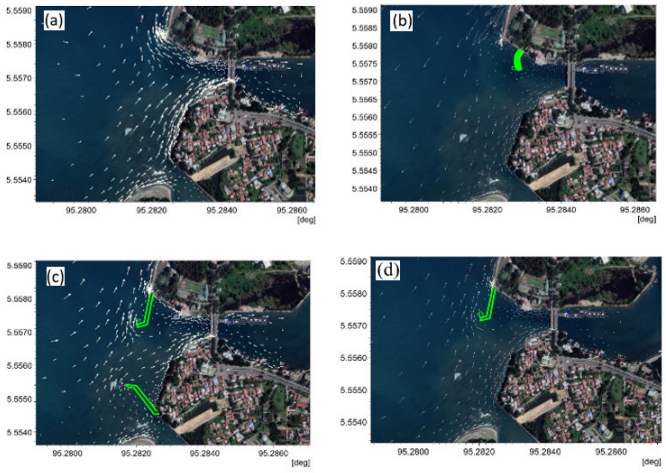

Source: Authors.

into the estuary, with some of the current subsequently shifting northward and flowing parallel to the coastline after passing under the bridge. This scenario created a circular current within the southern breakwater, potentially increasing sedimentation.

Scenario 3 (Figure 4d) resulted in a maximum current of 7.9 cm/s. The water mass from the south moved into the estuary, and under the bridge, it deflected counterclockwise towards the breakwater. This deflection caused the current in front of the pier to move westward towards the breakwater, leading to a reduction in its strength.

In general, the presence of breakwater structures in scenarios 1, 2, and 3 effectively reduced the current velocity compared to the existing conditions without breakwaters (Figure 5a). This occurs because when the water flow encounters the breakwater, it decelerates and changes direction, leading to the dissipation of kinetic energy and a subsequent decrease in current velocity (Le Xuan et al., 2024). Figure 5b visually represents the extent of this reduction using the existing scenario as a baseline for the maximum and average current values in each scenario. Among the three scenarios, Scenario 1 demonstrated the most significant reduction, with a 19% decrease in the maximum current velocity, along with the highest reduction in the average current, compared with scenarios 2 and 3. Scenario 2 achieved an 11% reduction in the maximum current speed, whereas scenario 3 achieved a 14% reduction. The inward curve of the structure in Scenario 1 is thought to improve harbor sheltering, minimize exposure to open-sea conditions, and result in a substantial reduction in harbor currents (Tsai et al., 2024). Therefore, the presence of a breakwater structure in the Ulee Lheue Harbor mitigates energy levels and reduces current velocities in the area.

Figure 5: Maximum and average current speed (a) and reduction percentage of the current speed for each scenario condition (b).

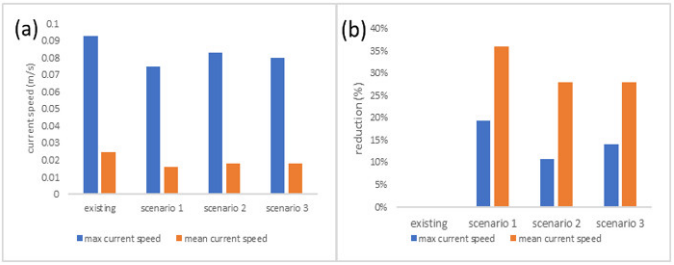

Source: Authors.

3.2. *Wave Height Mitigation.*

Waves in Banda Aceh generally originate from the northwest and follow the coastline as they approach the Ulee Lheue Beach. The Ulee Lheue Port is situated within the mouth of an estuary, a natural feature that diminishes wave intensity and reduces wave heights in the surrounding waters.

Under existing conditions, the wave height in front of the fishing port ranged from 7.37 to 14.56 cm, with an average significant wave height of 10.03 cm (Figure 6a). The introduction of the structure in Scenario 1 (Figure 6b) led to a reduction in wave height, with recorded wave heights ranging from 2.9 cm to 12.3 cm and an average wave height of 4.6 cm. In Scenario 2 (Figure 6c), the wave height varied from 0.8 cm to 12.3 cm, with an average height of 3.5 cm, while in Scenario 3 (Figure 6d), the wave height ranged from 0.7 cm to 13.3 cm, with an average height of 3.7 cm.

Figure 6: Wave height conditions towards full tide for existing conditions without structure (a), scenario 1 structure (b), scenario 2 structure (c), and scenario 3 structure (d).

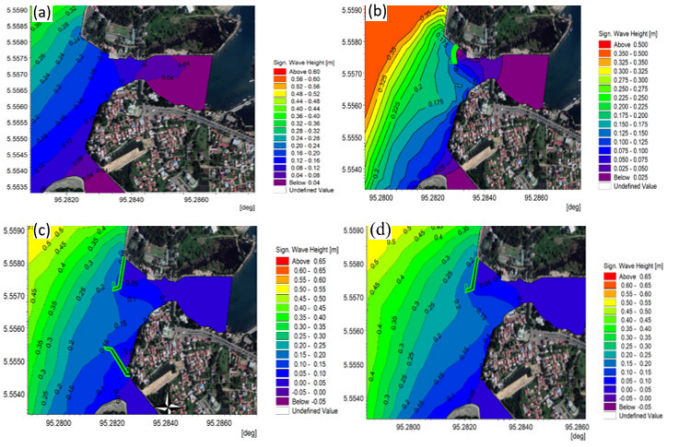

Source: Authors.

These structures function as barriers that intercept incoming waves. When waves encounter these structures, they slow down and change direction. The structures also played a role in wave reflection. In Scenario 2, where the structure covers a larger portion of the harbor entrance, it effectively reflects a significant

portion of the incoming wave energy back towards the open sea. These combined effects result in a substantial reduction in the wave height, effectively mitigating waves around the jetty.

The direction and height of the waves at the jetty are illustrated using wave rosettes in Figure 7. Under the existing conditions (Figure 7a), the waves impacting the fishing pier structure predominantly originate from the west, with 60% of the wave events coming from this direction, whereas 40% originate from the southwest. The dominant wave height from each direction was less than 0.2 meters. In Scenario 1 (Figure 7b), the introduction of additional structures reduced the maximum wave height to approximately 0.1 meters. In Scenarios 2 (Figure 7c) and 3 (Figure 7d), the dominant wave direction shifted to the southwest, with the predominant wave height further reduced to less than 0.05 meters.

Figure 7: Wave roses at full tide in front of the fishing port jetty under (a) existing conditions without a breakwater, (b) scenario structure 1, (c) plan structure 2, and (d) plan structure 3.

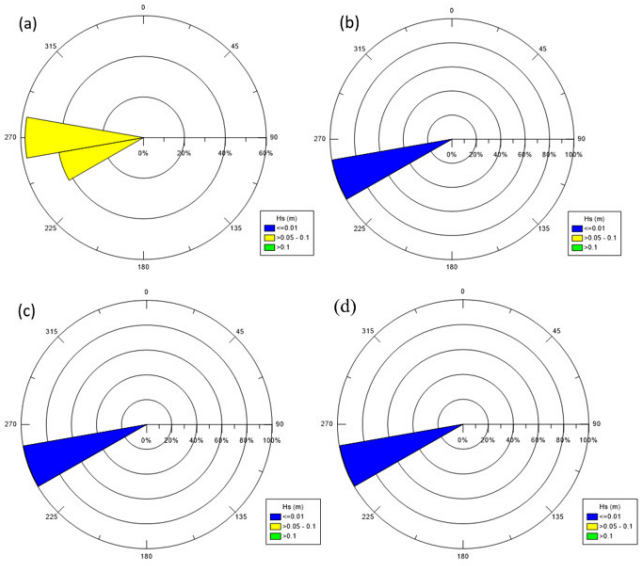

Source: Authors.

3.3. Energy Dissipation Analysis.

The wave energy intensity and significant wave height at sea showed considerable variability and were influenced by seasonal changes and weather conditions, resulting in a wide range of observed values. There is a directly proportional relationship between the wave energy and significant wave height (Chen et al., 2023) in front of the Ulee Lheue Port, as illustrated in Figure 8a. Under existing conditions, the significant wave energy varied from 0.01107 to 0.0272 kW/m, with an average value of 0.0186 kW/m, corresponding to wave heights ranging from 0.074 to 0.16 meters.

The implementation of the structures in Scenario 1 reduced the wave energy significantly, with values ranging from 0.00153 to 0.01334 kW/m, averaging 0.00385 kW/m. In contrast, Scenario 2 yielded an average energy of 0.00247 kW/m, whereas Scenario 3 yielded an average energy of 0.027 kW/m. As shown in Figure 8b, the significant wave energy in the existing condition was consistently higher than that in scenarios involving structural modifications. Interestingly, an upward trend in wave energy was observed around October, coinciding with the seasonal transition in Banda Aceh, when strong winds from the northeast exposed the Ulee Lheue area to larger waves (Rizal et al., 2012; Setiawan et al., 2018).

Figure 8c further illustrates the inverse relationship between the significant wave height and the peak wave period. A higher significant wave height generally corresponded to a shorter peak wave period. Under existing conditions, both the significant wave height and peak wave period were higher than those in scenarios 1, 2, and 3. The wave periods under the existing conditions also exhibited a broader range of values. However, the presence of structures in these scenarios resulted in lower significant wave heights and shorter wave periods. Scenario 2, in particular, proved to be more effective in mitigating wave impacts at Ulee Lheue Port. The dual structures in Scenario 2 provided enhanced protection, particularly during seasons when waves approached from multiple directions. This approach ensures that the inner port area remains secure irrespective of the direction of incoming waves, offering robust protection against potential maritime.

Figure 8: Percentage of wave power reduction for each scenario condition compared to existing conditions.

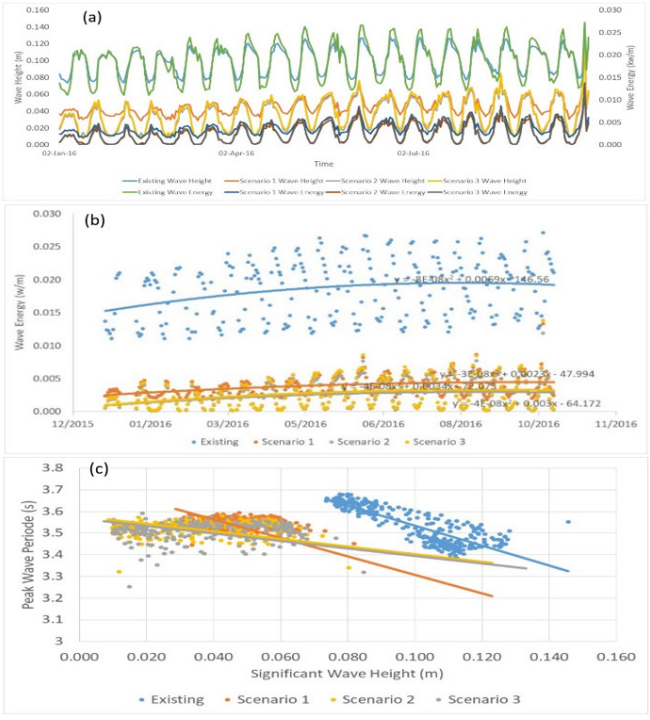

Source: Authors.

As previously discussed, there is a direct correlation between the significant wave height and energy generated, which is clearly reflected in the high wave energy values under the current conditions (see Figure 9). The introduction of structures in scenarios 1, 2, and 3 resulted in substantial reductions of 51

%, 56 %, and 49 %, respectively, in the maximum significant wave height around the fishing port. Additionally, the mean significant wave height decreased significantly, with reductions of 79%, 87%, and 85% in scenarios 1, 2, and 3, respectively.

Figure 9: Comparison of parametric (a) wave height and energy (b) wave energy (c) peak wave period and significant wave height.

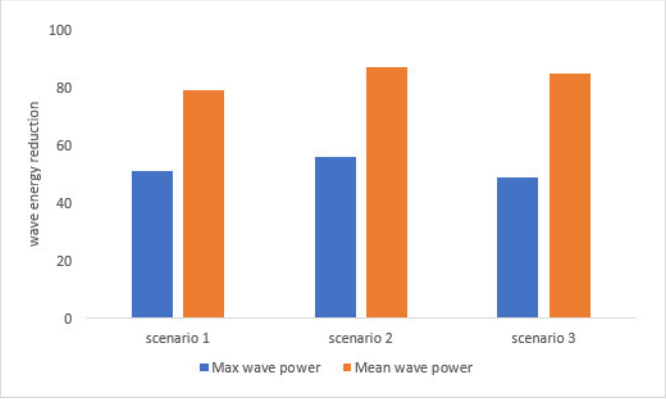

Source: Authors.

These findings indicate that the use of structures in the Ulee Lheue is highly effective in mitigating wave energy in the port area, leading to a significant reduction in wave energy compared with existing conditions. Notably, Scenario 2 proved to be the most effective, offering the greatest protection because of the presence of two structures that shielded the harbor from incoming waves. The dual-structure configuration in Scenario 2 is particularly effective in providing sheltered conditions within the Ulee Lheue Port, ensuring enhanced protection against wave impacts.

Conclusions.

The implementation of breakwater structures in the Ulee Lheue Estuary has demonstrated significant effectiveness in mitigating the wave energy and current velocities within the port area. A comparative analysis of the three scenarios revealed that Scenario 2, featuring dual impermeable structures, yielded the most substantial reduction in wave power, achieving an 87% decrease in the average wave energy. This configuration effectively shielded the Ulee Lheue Port from incoming waves, providing enhanced protection and improving the operational efficiency. These findings underscore the critical role of well-designed breakwater structures in safeguarding coastal infrastructures in wave-exposed environments. The results offer valuable insights for future planning and implementation of coastal protection measures in similar locations.

References.

Abood, K.A., Metzger, S.G., Distante, D.F., 1999. Minimizing dredging disposal via sediment management in New York harbor. Estuaries 22, 763–769. https://doi.org/10.2307/13-53109.

Ahn, J., Na, Y., Park, S.W., 2019. Development of Two-Dimensional Inundation Modelling Process using MIKE21 Model. KSCE J. Civ. Eng. 23, 3968–3977. https://doi.org/10.1007-/s12205-019-1586-9.

Akbari, H., Karami Matin, A.A., Shafieefar, M., 2022. The effect of sequential storms on the performance of homogeneous berm breakwaters. Coast. Eng. 175, 104141. https://doi.org/10.-1016/j.coastaleng.2022.104141.

Archetti, R., Zanuttigh, B., 2010. Integrated monitoring of the hydro-morphodynamics of a beach protected by low crested detached breakwaters. Coast. Eng. 57, 879–891. https://doi.org/-10.1016/j.coastaleng.2010.05.002.

Chen, Y., Zhang, D., Li, X., Peng, Y., Wu, C., Pu, H., Zhou, D., Cao, Y., Zhang, J., 2023. Significant wave height prediction through artificial intelligent mode decomposition for wave energy management. Energy AI 14, 100257. https://doi.org/10.10-16/j.egyai.2023.100257.

Cui, J., Chen, X., Sun, P., 2021. Numerical investigation on the hydrodynamic performance of a new designed breakwater using smoothed particle hydrodynamic method. Eng. Anal. Bound. Elem. 130, 379–403. https://doi.org/10.1016/J.ENGA-NABOUND.2021.05.007.

Dev, S.G.D., Deepchand, V., Anoop, M.S., Krishnaprasad, P.K., Nazeer, M.N., Singh, Y., Arjun, S., Prasanth, R.S., 2023. Influence of a fishing harbour on coastal geomorphology of the southwest coast of India and predictions of its future trends. Geosystems and Geoenvironment 2, 100179. https://doi.org/10-.1016/J.GEOGEO.2023.100179.

Fadli, N., Syafruddin, S., Hasibuan, P., Sofyan, S.E., Rianjuanda, R., Syukri, M., Saidi, T., Dawood, R., 2021. Composition and catch number of fish landings on the eastern coast of the Aceh region. IOP Conf. Ser. Earth Environ. Sci. 674, 12074. https://doi.org/10.1088/1755-1315/674/1/012074.

Fatimah, E., Fauzi, A., 2021. Analisis Pergerakan Arus Pasang Surut terhadap Perubahan Perletakan Pemecah Ombak di Pelabuhan Ulee Lheue. J. Tek. Sipil 10, 1–8. https://doi.org/-10.24815/jts.v10i1.18980.

Feng, B., Li, Z., Lu, H., Yan, Y., Hou, G., 2024. Estimating the total allowable catch and management of Threadfin porgy (Evynnis cardinalis) fisheries in the northern South China Sea based on sampling surveys conducted at fishing ports. Aquac. Fish. 9, 273–279. https://doi.org/https://doi.org/10.1016/j.aaf.-2021.12.003.

Gao, J., Ji, C., Liu, Y., Ma, X., Gaidai, O., 2017. Influence of offshore topography on the amplification of infragravity oscillations within a harbor. Appl. Ocean Res. 65, 129–141. https://doi.org/10.1016/j.apor.2017.04.001.

Ghose, D.K., Panda, S.S., Swain, P.C., 2010. Prediction of water table depth in western region, Orissa using BPNN and RBFN neural networks. J. Hydrol. 394, 296–304. https://doi.-org/10.1016/J.JHYDROL.2010.09.003.

Guler, H.G., Kirezci, C., Baykal, C., Tarakcioglu, G.O., Isik, E., Ergin, A., Yalciner, A.C., Guler, I., 2024. Storm damage assessment of a port in the Southwestern Black Sea. Coast.

Eng. 192, 104544. https://doi.org/https://doi.org/10.1016/j.-coastaleng.2024.104544.

Haditiar, Y., Ikhwan, M., Mahdi, S., Siregar, A.N., Haridhi, H.A., Setiawan, I., Nanda, M., Prajaputra, V., Irham, M., 2024. Oceanographic characteristics in the North of Aceh waters. Reg. Stud. Mar. Sci. 71, 103408. https://doi.org/https:// doi.org/10.-1016/j.rsma.2024.103408.

Haridhi, H., Nanda, M., Haditiar, Y., Rizal, S., 2018. Application of Rapid Appraisals of Fisheries Management System (RAFMS) to identify the seasonal variation of fishing ground locations and its corresponding fish species availability at Aceh waters, Indonesia. Ocean Coast. Manag. 154, 46–54. https://-doi.org/10.1016/j.ocecoaman.2017.12.030.

Hou, W., Zhang, R., Zhang, P., Xi, Y., Ma, Q., 2021. Wave Characteristics and Berthing Capacity Evaluation of the Offshore Fishing Port under the Influence of Typhoons. Appl. Ocean Res. 106, 102447. https://doi.org/10.1016/J.APOR.20-20.102447.

Hsu, T.W., Hsieh, C.M., Hwang, R.R., 2004. Using RANS to simulate vortex generation and dissipation around impermeable submerged double breakwaters. Coast. Eng. 51, 557–579. https://doi.org/10.1016/J.COASTALENG.2004.06.003.

Huang, C.J., Chang, H.H., Hwung, H.H., 2003. Structural permeability effects on the interaction of a solitary wave and a submerged breakwater. Coast. Eng. 49, 1–24. https://doi.org/10-.1016/S0378-3839(03)00034-6.

Kim, D.H., Kim, Y.J., Hur, D.S., 2014. Artificial neural network based breakwater damage estimation considering tidal level variation. Ocean Eng. 87, 185–190. https://doi.org/10.10-16/J.OCEANENG.2014.06.001.

Le Xuan, T., Vu, H.T.D., Oberle, P., Dang, T.D., Tran Ba, H., Le Manh, H., 2024. Hydrodynamics and wave transmission through a hollow triangle breakwater. Estuar. Coast. Shelf Sci. 302, 108765. https://doi.org/10.1016/j.ecss.2024.108765.

López, M., Iglesias, G., 2014. Long wave effects on a vessel at berth. Appl. Ocean Res. 47, 63–72. https://doi.org/10.1016/-J.APOR.2014.03.008N'.

Souvi, K., Sun, C., Rivero Rivero, Y.M., 2023. Development of marine small-scale fisheries in Togo: An examination of the efficiency of fishermen at the new fishing port of Lomé and the necessity of fisheries co-management. Aquac. Fish. https://doi.org/https://doi.org/10.1016/j.aaf.2023.07.009.

Ondara, K., Rahmawan, G.A., Gemilang, W.A., Wisha, U.J., Dhiauddin, R., 2018. Numerical hydrodynamic wave modelling using spatial discretization in Brebes waters, Central Java, Indonesia. Int. J. Adv. Sci. Eng. Inf. Technol. https://doi.org/1-0.18517/ijaseit.8.1.4166.

Paravath, K., Parth, J., Nasar, T., 2021. Geomorphologic Impact of Construction of Breakwaters at Ponnani Fishery Harbour in Kerala. IOP Conf. Ser. Earth Environ. Sci. 809. https://doi.org/10.1088/1755-1315/809/1/012016.

Pradhan, U.K., Mishra, P., Mohanty, P.K., Panda, U.S., Ramanamurthy, M. V., 2020. Modeling of tidal circulation and sediment transport near tropical estuary, east coast of India. Reg. Stud. Mar. Sci. 37, 101351. https://doi.org/10.1016/J.RS-MA.2020.101351.

Purnawan, S., Karina, S., Kang, M., Manik, H., 2023. Fish Stock Status Assessment in Alue Naga Waters Using A 200 Khz Single Beam Echosounder. ILMU Kelaut. Indones. J. Mar. Sci. 28, 57–68. https://doi.org/10.14710/ik.ijms.28.1.57-68.

Rahmawan, G., Ondara, K., Adnan, I., 2021. Pemetaan Morfologi Dasar Perairan Untuk Pemantauan Sedimentasi di Dermaga Perikanan Ulee Lheu Menggunakan Single Beam Odometer Dua Frekuensi. J. Kelaut. Indones. J. Mar. Sci. Technol. 14, 143–148. https://doi.org/10.21107/jk.v14i2.10317.

Rizal, S., Damm, P., Wahid, M.A., Sündermann, J., Ilhamsyah, Y., Iskandar, T., Muhammad, 2012. General circulation in the Malacca Strait and Andaman Sea: A numerical model study. Am. J. Environ. Sci. 8, 479–488. https://doi.org/10.3844-/ajessp.2012.479.488.

Romano-Moreno, E., Diaz-Hernandez, G., L. Lara, J., Tomás, A., F. Jaime, F., 2022. Wave downscaling strategies for practical wave agitation studies in harbours. Coast. Eng. 175, 104140. https://doi.org/10.1016/j.coastaleng.2022.104140.

Rupali, Kumar, P., 2021. Mathematical modeling of arbitrary shaped harbor with permeable and impermeable breakwaters using hybrid finite element method. Ocean Eng. 221, 108551. https://doi.org/10.1016/J.OCEANENG.2020.108551.

Samaras, A., Vacchi, M., Archetti, R., Lamberti, A., 2013. Wave and hydrodynamics modelling in coastal areas with TELEMAC and MIKE21, in: XXth TELEMAC-MASCARET User Conference. pp. 59–63.

Setiawan, I., Rizal, S., Haditiar, Y., Ilhamsyah, Y., Purnawan, S., Irham, M., Yuni, S.M., 2018. Study of current circulation in the Northern Waters of Aceh, in: IOP Conference Series: Earth and Environmental Science. https://doi.org/10.1088-/1755-1315/176/1/012016.

Takagi, H., Goda, Y., 2000. A Reliability Design Method of Caisson Breakwaters with Optimal Wave Heights. Coast. Eng. J. Vol.42, pp.357-387. https://doi.org/10.1016/S0578-5634(00)-00018-3.

Thaib, R., Rizwan, T., Mauliza, T., Setiawan, I., El-Rahimi, S.A., 2024. Analysis of Fishermen Satisfaction Level at Ujong Baroh Fishing Port, Aceh, Indonesia. J. Marit. Res. 21, 30–35.

Tsai, C.-P., Ko, C.-H., Shih, H.-C., Chen, Y.-H., Chen, Y.-C., 2024. Comparative study of wave height transformation: Bragg reflection versus wave breaking at submerged rectangular breakwaters. Ocean Eng. 299, 117277. https://doi.org/10.-1016/j.oceaneng.2024.117277.

Wang, B., Reeve, D., 2010. Probabilistic modelling of long-term beach evolution near segmented shore-parallel breakwaters. Coast. Eng. 57, 732–744. https://doi.org/10.1016/j.coast-aleng.2010.03.004.

Zhao, X., Li, Y., Zou, Q., Han, D., Geng, J., 2022. Long wave absorption by a dual purpose Helmholtz resonance OWC breakwater. Coast. Eng. 178. https://doi.org/10.1016/j.coast-aleng.2022.104203.

Zhou, T., Yin, Y., Ma, Z., Chen, J., Zhai, G., 2023. Numerical investigation of breaking waves impact on vertical breakwater with impermeable and porous foundation. Ocean Eng. 280, 114477. https://doi.org/https://doi.org/10.1016/j.oceaneng.2023-.114477.